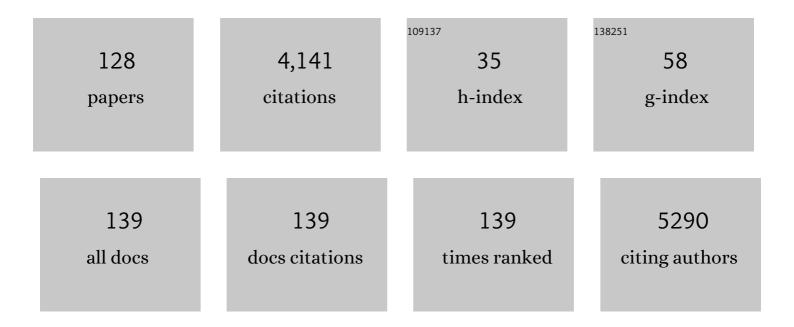
## Mohamed Mokhtar M Mostafa

List of Publications by Year in descending order

Source: https://exaly.com/author-pdf/2679374/publications.pdf Version: 2024-02-01



#	Article	IF	CITATIONS
1	New green perspective to dihydropyridines synthesis utilizing modified heteropoly acid catalysts. Catalysis Today, 2022, 397-399, 484-496.	2.2	9
2	Noble metal (Pd, Pt and Rh) incorporated LaFeO3 perovskite oxides for catalytic oxidative cracking of n-propane. Catalysis Today, 2022, 397-399, 81-93.	2.2	8
3	Enhanced stability of SrRuO3 mixed oxide via monovalent doping in Sr1-xKxRuO3 for the oxygen evolution reaction. Journal of Power Sources, 2022, 521, 230950.	4.0	15
4	MoOx and WOx conjugated iron phosphate nanotubes catalysts for benzylation of benzene using benzyl alcohol. Catalysis Communications, 2022, 164, 106423.	1.6	3
5	Metal Oxides as Catalyst/Supporter for CO2 Capture and Conversion, Review. Catalysts, 2022, 12, 300.	1.6	41
6	Synthesis and characterization of hexagonal Mg Fe layered double hydroxide/grapheme oxide nanocomposite for efficient adsorptive removal of cadmium ion from aqueous solutions: Isotherm, kinetic, thermodynamic and mechanism. Journal of Water Process Engineering, 2022, 47, 102746.	2.6	39
7	Fe3O4@date seeds powder: a sustainable nanocomposite material for wastewater treatment. Journal of Materials Research and Technology, 2022, 18, 3581-3597.	2.6	14
8	Câ^'H Methylation Using Sustainable Approaches. Catalysts, 2022, 12, 510.	1.6	4
9	Synthesis and Characterization of Green ZnO@polynaniline/Bentonite Tripartite Structure (G.Zn@PN/BE) as Adsorbent for As (V) Ions: Integration, Steric, and Energetic Properties. Polymers, 2022, 14, 2329.	2.0	34
10	Removal of bismuth ions utilizing pillared ilerite nanoclay: Kinetic thermodynamic studies and environmental application. Microporous and Mesoporous Materials, 2021, 313, 110826.	2.2	10
11	How oxidation state and lattice distortion influence the oxygen evolution activity in acid of iridium double perovskites. Journal of Materials Chemistry A, 2021, 9, 2980-2990.	5.2	36
12	Cu, Fe and Mn oxides intercalated SiO2 pillared magadiite and ilerite catalysts for NO decomposition. Applied Catalysis A: General, 2021, 616, 118100.	2.2	10
13	Synergistic Effect of NiLDH@YZ Hybrid and Mechanochemical Agitation on Glaser Homocoupling Reaction. Chemistry - A European Journal, 2021, 27, 8875-8885.	1.7	12
14	Supported Metal Nanoparticles Assisted Catalysis: A Broad Concept in Functionalization of Ubiquitous Câ''H Bonds. ChemCatChem, 2021, 13, 4655-4678.	1.8	13
15	Insight into the role of the zeolitization process in enhancing the adsorption performance of kaolinite/diatomite geopolymer for effective retention of Sr (II) ions; batch and column studies. Journal of Environmental Management, 2021, 294, 112984.	3.8	26
16	Transitionâ€Metalâ€Catalyzed Selective Alkynylation of Câ^'H Bonds. Advanced Synthesis and Catalysis, 2021, 363, 4994-5027.	2.1	26
17	Synthesis of zeolite/geopolymer composite for enhanced sequestration of phosphate (PO43â^') and ammonium (NH4+) ions; equilibrium properties and realistic study. Journal of Environmental Management, 2021, 300, 113723.	3.8	19
18	C–CN bond formation: an overview of diverse strategies. Chemical Communications, 2021, 57, 2210-2232.	2.2	38

#	Article	IF	CITATIONS
19	Design and green synthesis of novel quinolinone derivatives of potential anti-breast cancer activity against MCF-7 cell line targeting multi-receptor tyrosine kinases. Journal of Enzyme Inhibition and Medicinal Chemistry, 2021, 36, 1453-1470.	2.5	9
20	Transition metal catalyzed C–H bond activation by <i>exo</i> -metallacycle intermediates. Chemical Communications, 2021, 57, 11885-11903.	2.2	7
21	Recent advances in the incorporation of CO <sub>2</sub> for C–H and C–C bond functionalization. Green Chemistry, 2021, 23, 9283-9317.	4.6	17
22	Effect of the Thermal Treatment of Fe/N/C Catalysts for the Oxygen Reduction Reaction Synthesized by Pyrolysis of Covalent Organic Frameworks. Industrial & Engineering Chemistry Research, 2021, 60, 18759-18769.	1.8	12
23	A Green Mechanochemical One-Pot Three-Component Domino Reaction Synthesis of Polysubstituted Azoloazines Containing Benzofuran Moiety: Cytotoxic Activity Against HePG2 Cell Lines. Polycyclic Aromatic Compounds, 2020, 40, 594-608.	1.4	4
24	Porous Fe2O3-ZrO2 and NiO-ZrO2 nanocomposites for catalytic N2O decomposition. Catalysis Today, 2020, 348, 166-176.	2.2	16
25	Highly Efficient Nanosized Mesoporous CuMgAl Ternary Oxide Catalyst for Nitro-Alcohol Synthesis: Ultrasound-Assisted Sustainable Green Perspective for the Henry Reaction. ACS Omega, 2020, 5, 6532-6544.	1.6	21
26	Ultrasonic-Assisted Michael Addition of Arylhalide to Activated Olefins Utilizing Nanosized CoMgAl-Layered Double Hydroxide Catalysts. Catalysts, 2020, 10, 220.	1.6	11
27	Establishing High Photocatalytic H <sub>2</sub> Evolution from Multiwalled Titanate Nanotubes. ChemCatChem, 2020, 12, 2951-2956.	1.8	15
28	Chitosan Decorated Copper Nanoparticles as Efficient Catalyst for Synthesis of Novel Quinoline Derivatives. Journal of Nanoscience and Nanotechnology, 2020, 20, 890-899.	0.9	12
29	Sequential Template Decomposition to Adjust the Performance of Imperfect Zeolite BEA Membranes. Chemie-Ingenieur-Technik, 2019, 91, 953-960.	0.4	2
30	Acetone Reaction with Hydrogen over Mesoporous Magnesium Oxide-Supported Rhodium Nanoparticles. Topics in Catalysis, 2019, 62, 795-804.	1.3	3
31	Novel Efficient Pdâ€Free Niâ€Layered Double Hydroxide Catalysts for a Suzuki C–C Coupling Reaction. ChemistrySelect, 2019, 4, 7904-7911.	0.7	11
32	Photocatalytic H <sub>2</sub> Evolution: Dealloying as Efficient Tool for the Fabrication of Rhâ€decorated TiO <sub>2</sub> Nanotubes. ChemCatChem, 2019, 11, 6258-6262.	1.8	12
33	Template Assisted Microwave Synthesis of rGO-ZrO <sub>2</sub> Composites: Efficient Photocatalysts Under Visible Light. Journal of Nanoscience and Nanotechnology, 2019, 19, 5177-5188.	0.9	15
34	H-ZSM-5 Materials Embedded in an Amorphous Silica Matrix: Highly Selective Catalysts for Propylene in Methanol-to-Olefin Process. Catalysts, 2019, 9, 364.	1.6	18
35	MgAl-Layered Double Hydroxide Solid Base Catalysts for Henry Reaction: A Green Protocol. Catalysts, 2018, 8, 133.	1.6	32
36	Supported Zeolite Beta Layers via an Organic Template-Free Preparation Route. Molecules, 2018, 23, 220.	1.7	4

#	Article	IF	CITATIONS
37	Ultraviolet Radiation Induced Dopant Loss in a TiO <sub>2</sub> Photocatalyst. ACS Catalysis, 2017, 7, 1485-1490.	5.5	18
38	Chemical Vapor Deposition Synthesis and Optical Properties of Nb <sub>2</sub> O <sub>5</sub> Thin Films with Hybrid Functional Theoretical Insight into the Band Structure and Band Gaps. ACS Applied Materials & Interfaces, 2017, 9, 18031-18038.	4.0	54
39	Graphene-oxide-supported CuAl and CoAl layered double hydroxides as enhanced catalysts for carbon-carbon coupling via Ullmann reaction. Journal of Solid State Chemistry, 2017, 246, 130-137.	1.4	48
40	Dopant stability in multifunctional doped TiO <sub>2</sub> 's under environmental UVA exposure. Environmental Science: Nano, 2017, 4, 1108-1113.	2.2	1
41	Structural and photocatalytic properties of precious metals modified TiO2-BEA zeolite composites. Molecular Catalysis, 2017, 441, 140-149.	1.0	26
42	Hybrid effects in graphene oxide/carbon nanotube-supported layered double hydroxides: enhancing the CO2 sorption properties. Carbon, 2017, 123, 616-627.	5.4	47
43	Influence of the Reaction Temperature on the Nature of the Active and Deactivating Species During Methanol-to-Olefins Conversion over H-SAPO-34. ACS Catalysis, 2017, 7, 5268-5281.	5.5	95
44	Solvent-Free Biginelli Reactions Catalyzed by Hierarchical Zeolite Utilizing a Ball Mill Technique: A Green Sustainable Process. Catalysts, 2017, 7, 84.	1.6	42
45	Application of Synthetic Layered Sodium Silicate Magadiite Nanosheets for Environmental Remediation of Methylene Blue Dye in Water. Materials, 2017, 10, 760.	1.3	35
46	Photocatalytic Degradation of Methylene Blue Dye in Water Using Pt/ZnO-MWCNT Under Visible Light. Nanoscience and Nanotechnology Letters, 2017, 9, 144-150.	0.4	11
47	Physico-Chemical and Catalytic Properties of Mesoporous CuO-ZrO2 Catalysts. Catalysts, 2016, 6, 57.	1.6	41
48	Anodic TiO <sub>2</sub> nanotube arrays directly grown on quartz glass used in front―and backâ€side irradiation configuration for photocatalytic H <sub>2</sub> generation. Physica Status Solidi (A) Applications and Materials Science, 2016, 213, 2733-2740.	0.8	10
49	Innenrücktitelbild: Initial Carbon-Carbon Bond Formation during the Early Stages of the Methanol-to-Olefin Process Proven by Zeolite-Trapped Acetate and Methyl Acetate (Angew. Chem.) Tj ETQq1 1	0.7846314	rgBo∂ /Overloc
50	Photocatalytic H <sub>2</sub> Generation Using Dewetted Pt-Decorated TiO <sub>2</sub> Nanotubes: Optimized Dewetting and Oxide Crystallization by a Multiple Annealing Process. Journal of Physical Chemistry C, 2016, 120, 15884-15892.	1.5	43
51	Graphene oxide/mixed metal oxide hybrid materials for enhanced adsorption desulfurization of liquid hydrocarbon fuels. Fuel, 2016, 181, 531-536.	3.4	78
52	Initial Carbon–Carbon Bond Formation during the Early Stages of the Methanolâ€ŧoâ€Olefin Process Proven by Zeoliteâ€Trapped Acetate and Methyl Acetate. Angewandte Chemie, 2016, 128, 16072-16077.	1.6	56
53	Initial Carbon–Carbon Bond Formation during the Early Stages of the Methanolâ€toâ€Olefin Process Proven by Zeoliteâ€Trapped Acetate and Methyl Acetate. Angewandte Chemie - International Edition, 2016, 55, 15840-15845.	7.2	170
54	High-temperature annealing of TiO <sub>2</sub> nanotube membranes for efficient dye-sensitized solar cells. Semiconductor Science and Technology, 2016, 31, 014010.	1.0	25

#	Article	IF	CITATIONS
55	Simple and efficient protocol for synthesis of pyrido[1,2-a]pyrimidin-4-one derivatives over solid heteropolyacid catalysts. RSC Advances, 2016, 6, 11921-11932.	1.7	15
56	Cross-linked single-walled carbon nanotube aerogel electrodes via reductive coupling chemistry. Journal of Materials Chemistry A, 2016, 4, 5385-5389.	5.2	33
57	Bismuth oxyhalides: synthesis, structure and photoelectrochemical activity. Chemical Science, 2016, 7, 4832-4841.	3.7	252
58	Photocatalytic Degradation of p-Nitrophenol in Aqueous Suspension by Using Graphene/ZrO <sub>2</sub> Catalysts. Nanoscience and Nanotechnology Letters, 2016, 8, 448-457.	0.4	19
59	Singleâ€Walled TiO <sub>2</sub> Nanotubes: Enhanced Carrierâ€Transport Properties by TiCl <sub>4</sub> Treatment. Chemistry - A European Journal, 2015, 21, 9204-9208.	1.7	25
60	Multifunctional Nanobiocomposite of Poly[(butylenes succinate)-co-adipate] and Clay. Journal of Nanoscience and Nanotechnology, 2015, 15, 2446-2450.	0.9	2
61	Viscoelastic Properties of Poly[(butylenes succinate)-co-adipate] Nanocomposites. Journal of Nanoscience and Nanotechnology, 2015, 15, 2312-2316.	0.9	0
62	Influence of the Reaction Temperature on the Nature of the Active and Deactivating Species during Methanol to Olefins Conversion over H-SSZ-13. ACS Catalysis, 2015, 5, 992-1003.	5.5	112
63	Synthesis and characterization of decanuclear Ln(III) cluster of mixed calix[8]arene-phosphonate ligands (Ln=Pr, Nd). Inorganic Chemistry Communication, 2015, 54, 34-37.	1.8	17
64	Bridging different Co <sub>4</sub> –calix[4]arene building blocks into grids, cages and 2D polymers with chiral camphoric acid. CrystEngComm, 2015, 17, 1750-1753.	1.3	29
65	Heteropolyacid generated on the surface of iron phosphate nanotubes: structure and catalytic activity studies. RSC Advances, 2015, 5, 63917-63929.	1.7	11
66	Pillared HMCM-36 zeolite catalyst for biodiesel production by esterification of palmitic acid. Journal of Molecular Catalysis A, 2015, 406, 159-167.	4.8	43
67	Use of Anodic TiO <sub>2</sub> Nanotube Layers as Mesoporous Scaffolds for Fabricating CH <sub>3</sub> NH <sub>3</sub> PbI <sub>3</sub> Perovskiteâ€Based Solid‧tate Solar Cells. ChemElectroChem, 2015, 2, 824-828.	1.7	39
68	Influence of crystal structure of nanosized ZrO2 on photocatalytic degradation of methyl orange. Nanoscale Research Letters, 2015, 10, 73.	3.1	377
69	Stepwise Construction of Extra-Large Heterometallic Calixarene-Based Cages. Inorganic Chemistry, 2015, 54, 3183-3188.	1.9	53
70	The use of time resolved aerosol assisted chemical vapour deposition in mapping metal oxide thin film growth and fine tuning functional properties. Journal of Materials Chemistry A, 2015, 3, 4811-4819.	5.2	5
71	Self-condensation of acetone over Mg–Al layered double hydroxide supported on multi-walled carbon nanotube catalysts. Journal of Molecular Catalysis A, 2015, 398, 50-57.	4.8	17
72	Joule Heating Characteristics of Emulsionâ€∓emplated Graphene Aerogels. Advanced Functional Materials, 2015, 25, 28-35.	7.8	99

#	Article	IF	CITATIONS
73	Nanostructured Mg–Al Hydrotalcite as Catalyst for Fine Chemical Synthesis. Journal of Nanoscience and Nanotechnology, 2014, 14, 1931-1946.	0.9	37
74	Single-Particle Spectroscopy of Alcohol-to-Olefins over SAPO-34 at Different Reaction Stages: Crystal Accessibility and Hydrocarbons Reactivity. ChemCatChem, 2014, 6, 667-667.	1.8	0
75	Ethanol to hydrocarbons using silver substituted polyoxometalates: Physicochemical and catalytic study. Journal of Industrial and Engineering Chemistry, 2014, 20, 46-53.	2.9	11
76	Unique Coldâ€Crystallization Behavior and Kinetics of Biodegradable Poly[(butylene succinate)â€co adipate] Nanocomposites: A High Speed Differential Scanning Calorimetry Study. Macromolecular Materials and Engineering, 2014, 299, 939-952.	1.7	14
77	Singleâ€Particle Spectroscopy of Alcoholâ€toâ€Olefins over SAPOâ€34 at Different Reaction Stages: Crystal Accessibility and Hydrocarbons Reactivity. ChemCatChem, 2014, 6, 772-783.	1.8	27
78	Single-catalyst particle spectroscopy of alcohol-to-olefins conversions: Comparison between SAPO-34 and SSZ-13. Catalysis Today, 2014, 226, 14-24.	2.2	50
79	Combined Operando UV/Vis/IR Spectroscopy Reveals the Role of Methoxy and Aromatic Species during the Methanolâ€toâ€Olefins Reaction over Hâ€5APOâ€34. ChemCatChem, 2014, 6, 3396-3408.	1.8	57
80	Alkali-Metal-Templated Assembly of Two High-Nuclearity Cobalt Clusters Based on Thiacalix[4]arene. Crystal Growth and Design, 2014, 14, 5865-5870.	1.4	16
81	A Series of d <sup>10</sup> Metal Clusters Constructed by 2,6-Bis[3-(pyrazin-2-yl)-1,2,4-triazolyl]pyridine: Crystal Structures and Unusual Luminescences. Crystal Growth and Design, 2014, 14, 5011-5018.	1.4	36
82	Nanosized iron and nickel oxide zirconia supported catalysts for benzylation of benzene: Role of metal oxide support interaction. Applied Catalysis A: General, 2014, 486, 19-31.	2.2	19
83	Ru–C–ZnO Composite Catalysts for the Synthesis of Methyl Isobutyl Ketone via Single Step Gas Phase Acetone Self-Condensation. Catalysis Letters, 2014, 144, 1278-1288.	1.4	10
84	Generalized Synthesis of Calixarene-Based High-Nuclearity M <sub>4<i>n</i></sub> Nanocages (M = Ni) Tj ETQo	10 0 0 rgB <sup>-</sup> 1.4 rgB <sup>-</sup>	T /Overlock 10
85	Iron oxide supported sulfated TiO2 nanotube catalysts for NO reduction with propane. Ceramics International, 2014, 40, 4039-4053.	2.3	16
86	Divalent Transition Metals Substituted LaFeO3 Perovskite Catalyst for Nitrous Oxide Decomposition. Journal of Membrane and Separation Technology, 2014, 3, 206-212.	0.4	10
87	Singleâ€Particle Spectroscopy on Large SAPOâ€34 Crystals at Work: Methanolâ€toâ€Olefin versus Ethanolâ€toâ€Olefin Processes. Chemistry - A European Journal, 2013, 19, 11204-11215.	1.7	54
88	Synthesis, characterization, and catalytic activity of nitridated magnesium silicate catalysts. Journal of Materials Science, 2013, 48, 4274-4283.	1.7	12
89	Microwave assisted efficient protocol for the classic Ullmann homocoupling reaction using Cu–Mg–Al hydrotalcite catalysts. Journal of Molecular Catalysis A, 2013, 379, 152-162.	4.8	29
90	Effect of synthesis methods for mesoporous zirconia on its structural and textural properties. Journal of Materials Science, 2013, 48, 2705-2713.	1.7	42

#	Article	IF	CITATIONS
91	Synthesis and characterization of partially crystalline nanosized ZSM-5 zeolites. Ceramics International, 2013, 39, 683-689.	2.3	23
92	An unusual silver–ethynide polymeric chain containing centrosymmetric Ag14 cluster segments stabilized by mixed carboxylate ligands. Inorganic Chemistry Communication, 2013, 31, 54-57.	1.8	6
93	Mg–Al hydrotalcite as an efficient catalyst for microwave assisted regioselective 1,3-dipolar cycloaddition of nitrilimines with the enaminone derivatives: A green protocol. Journal of Molecular Catalysis A, 2013, 367, 12-22.	4.8	28
94	Nano Cu Metal Doped on TiO <sub>2</sub> –SiO <sub>2</sub> Nanoparticle Catalysts in Photocatalytic Degradation of Direct Blue Dye. Journal of Nanoscience and Nanotechnology, 2013, 13, 4975-4980.	0.9	16
95	Layered double hydroxides supported on multi-walled carbon nanotubes: preparation and CO2 adsorption characteristics. Journal of Materials Chemistry, 2012, 22, 13932.	6.7	92
96	Effect of iron oxide loading on the phase transformation and physicochemical properties of nanosized mesoporous ZrO2. Materials Research Bulletin, 2012, 47, 3463-3472.	2.7	37
97	Graphene Oxide as Support for Layered Double Hydroxides: Enhancing the CO <sub>2</sub> Adsorption Capacity. Chemistry of Materials, 2012, 24, 4531-4539.	3.2	205
98	Mg–Al hydrotalcites as efficient catalysts for aza-Michael addition reaction: A green protocol. Journal of Molecular Catalysis A, 2012, 353-354, 122-131.	4.8	62
99	Activation and local structural stability during the thermal decomposition of Mg/Al-hydrotalcite by total neutron scattering. Journal of Materials Chemistry, 2011, 21, 15479.	6.7	22
100	An eco-friendly N-sulfonylation of amines using stable and reusable Zn–Al–hydrotalcite solid base catalyst under ultrasound irradiation. Ultrasonics Sonochemistry, 2011, 18, 172-176.	3.8	42
101	Structural, magnetic and electrical properties of Ga-substituted NiCuZn nanocrystalline ferrite. Ceramics International, 2010, 36, 1339-1346.	2.3	34
102	Nanosized spinel oxide catalysts for CO-oxidation prepared via CoMnMgAl quaternary hydrotalcite route. Journal of Alloys and Compounds, 2010, 493, 376-384.	2.8	43
103	Effect of Zr4+ doping on the stabilization of ZnCo-mixed oxide spinel system and its catalytic activity towards N2O decomposition. Journal of Alloys and Compounds, 2010, 493, 630-635.	2.8	20
104	Copper substituted heteropolyacid catalysts for the selective dehydration of ethanol. Journal of Alloys and Compounds, 2010, 496, 553-559.	2.8	22
105	Removal of chlorophenol from aqueous solutions by multi-walled carbon nanotubes: Kinetic and thermodynamic studies. Journal of Alloys and Compounds, 2010, 500, 87-92.	2.8	53
106	Thermal decomposition, gas phase hydration and liquid phase reconstruction in the system Mg/Al hydrotalcite/mixed oxide: A comparative study. Applied Clay Science, 2010, 50, 176-181.	2.6	64
107	Physicochemical and texture properties of nanocrystalline ZnCo <sub>2</sub> O <sub>4</sub> spinel and effect of <i>γ</i> -irradiation on its sintering process. Materials Technology, 2009, 24, 100-104.	1.5	3
108	Modification of surface and catalytic properties of Cu nanostructure catalysts used in methanol synthesis and steam reforming. International Journal of Nanoparticles, 2009, 2, 156.	0.1	0

#	Article	IF	CITATIONS
109	Preparation and physicochemical characterisation of thermally stable nano-sized hopcalite catalysts. International Journal of Nanomanufacturing, 2009, 4, 159.	0.3	2
110	Chemical modification of multi-walled carbon nanotubes using different oxidising agents: optimisation and characterisation. International Journal of Nanoparticles, 2009, 2, 200.	0.1	6
111	Effect of Li2O and CoO-doping of CuO/Fe2O3 system on its surface and catalytic properties. Applied Surface Science, 2007, 253, 9407-9413.	3.1	19
112	Structure and electrical transport properties of pure and Li2O-doped CuO/MgO solid solution. Materials Research Bulletin, 2005, 40, 891-902.	2.7	7
113	Electrical properties of pure and Li2O-doped NiO/MgO system. Solid State Ionics, 2004, 170, 33-42.	1.3	15
114	Thermal behaviour of ammonium molybdate-basic magnesium carbonate system doped with lithium nitrate. Journal of Thermal Analysis and Calorimetry, 2003, 71, 977-986.	2.0	4
115	Surface and catalytic properties of CuO and Co3O4 solids as influenced by treatment with Co2+ and Cu2+ species. Applied Catalysis A: General, 2003, 241, 77-90.	2.2	38
116	Surface and Catalytic Properties of the CuO/Al2O3 System as Influenced by Treating with Trace Amounts of MoO3. Adsorption Science and Technology, 2003, 21, 425-438.	1,5	3
117	Surface and catalytic properties of CuO doped with Li2O and Al2O3. Colloids and Surfaces A: Physicochemical and Engineering Aspects, 2002, 203, 205-215.	2.3	10
118	Surface and Catalytic Properties of the Co3O4/MgO System Doped with Fe2O3. Adsorption Science and Technology, 2001, 19, 621-634.	1,5	2
119	Surface and Catalytic Properties of the γ-Irradiated ZnO-Treated Co3O4/Al2O3 System. Adsorption Science and Technology, 2001, 19, 751-763.	1.5	6
120	Hydrogenolysis of Dimethyl Maleate on Cu/ZnO/Al2O3 Catalysts. Chemical Engineering and Technology, 2001, 24, 423-426.	0.9	41
121	Effect of MgO-doping on solid–solid interactions in MoO3/Al2O3 system. Thermochimica Acta, 1999, 327, 39-46.	1.2	26
122	Solid–solid interaction in CuO–ZnO/Al2O3 system under varying conditions. Thermochimica Acta, 1998, 319, 67-74.	1.2	13
123	Effects of Li2O doping on surface and catalytic properties of CuO–ZnO/Al2O3 system. Colloids and Surfaces A: Physicochemical and Engineering Aspects, 1998, 142, 17-25.	2.3	32
124	Physicochemical Surface and Catalytic Properties of the Na <sub>2</sub> O-doped CuO–ZnO/Al <sub>2</sub> O <sub>3</sub> System. Adsorption Science and Technology, 1998, 16, 77-86.	1.5	9
125	Effect of gamma-irradiation on surface and catalytic properties of CuOâ^'ZnO/Al2O3 system. Journal of Radioanalytical and Nuclear Chemistry, 1997, 219, 89-94.	0.7	37
126	Effect of ZnO on surface and catalytic properties of CuOAl2O3 system. Applied Catalysis A: General, 1997, 155, 167-178.	2.2	67

#	Article	IF	CITATIONS
127	Analysis of thermally induced solid-solid interactions in vanadia-alumina system. Journal of Thermal Analysis, 1996, 46, 1473-1481.	0.7	9
128	Hexagonal Mg-Fe Ldh and Graphene Oxide Nanocomposite for Efficient Removal of Cd(Ii) from Aqueous Solutions. SSRN Electronic Journal, 0, , .	0.4	0